Electronic Supplementary Information

Ultrathin rhodium nanosheets-gold nanowires nanocomposites for alkaline methanol oxidation reaction

Bin Sun,[a] Zhe Wang,[a] Zi-Han Yuan,[a] Yu Ding,[a] Fu-Min Li,*[b] Guang-Tao Zhao,*[a] Dong-Sheng Li,[c] Xi-Fei Li[d] and Yu Chen*[a]

[a] *Key Laboratory of Macromolecular Science of Shaanxi Province, Shaanxi Key Laboratory for Advanced Energy Devices, Shaanxi Engineering Lab for Advanced Energy Technology, School of Materials Science and Engineering, Shaanxi Normal University, Xi'an 710062, PR China. Email: ndchenyu@gmail.com (Y. Chen); zhaoguangtao@snnu.edu.cn (G. T. Zhao)*

[b] *School of Chemistry and Chemical Engineering, Huazhong University of Science and Technology, Wuhan 430074, Hubei, PR China. Email: lifuminxs@gmail.com (F. M. Li)*

[c] *College of Materials and Chemical Engineering, Key Laboratory of Inorganic Nonmetallic Crystalline and Energy Conversion Materials, China Three Gorges University, Yichang 443002, PR China.*

[d] *Key Laboratory of Advanced Batteries Materials for Electric Vehicles of China Petroleum and Chemical Industry Federation, School of Materials Science and Engineering, Xi'an University of Technology, Xi'an 710048, PR China.*

Experimental section

Reagents and chemicals

Rhodium(III) 2,4-pentanedionate ($Rh(acac)_3$, 97%) were purchased from Shanghai Macklin Biochemical Co., Ltd. (Shanghai, China). Polyvinylpyrrolidone (PVP, K30), acetone and formaldehyde aqueous solution were purchased from Sinopharm Chemical Reagent Co., Ltd. (Shanghai, China). Benzyl alcohol were purchased from Guangzhou Jinhuada Chemical Reagent Co., Ltd. Chloroauric acid ($HAuCl_4$), 1-naphthol ($C_{10}H_8O$) were supplied by Aladdin-Holdings Group Co., Ltd. All regents were used as received without further purification.

Synthesis of catalysts

Synthesis of ultrathin Rh nanosheets (Rh NSs). $Rh(acac)_3$ (8.0 mg) and PVP (K30, 120.0 mg) were dissolved in a mixed solution of benzyl alcohol and formaldehyde (6 mL, $V_{benzyl\ alcohol} = V_{formaldehyde}$). Using an ultrasound machine for 10 minutes to blend the mixture evenly. It was then transferred to a high pressure reaction kettle lined with teflon and kept at 180°C for 8 hours before being cooled to room temperature.

Synthesis of gold nanowires (Au NWs). $HAuCl_4$ (1mL 0.029 M), 1-naphthol (1 mL 0.5 M) were dissolved in a ethanol solution (8 mL, $V_{water} = V_{ethanol}$), which was further held at 30℃ for 2 h.

Rh NSs-Au NWs nanocomposites (Rh-Au CNSs). Rh NSs and Au NWs were mixed under ultrasound for 10 minutes. The obtained Rh-Au CNSs was further subjected to ultraviolet ozone treatment on UVO-6 for 10 h to remove all organic species on their surface. The final product is dried under vacuum.

Electrochemical measurements.

CV and chronopotentiometry results were obtained from a electrochemical analyzer (CHI-660) at 30 ± 1℃. Based on a three-electrode system, a carbon rod with 5 mm diameter served as an auxiliary electrode, a saturated calomel electrode was used as a reference electrode, and the working electrode was an catalyst-modified glassy carbon. The electrocatalyst ink was prepared by dispersing 5 mg of catalysts in a mixed solution of water and isopropyl alcohol (2.5 mL, $V_{water} : V_{isopropyl\ alcohol} = 4 : 1$). 4 μL of catalyst

ink was loaded onto the glassy carbon electrode with a loading of 0.114 mg $cm^{-2}$and dried in the drying oven at 60℃. Then, 3 μL of Nafion solution (0.05 wt%) was further coated on the catalyst surface and dried at 60℃.

Physical characterization.

Powder X-ray diffraction (XRD) results were recorded on SmartLab (9) instrument at room temperature. Scanning electron microscopy (SEM) measurements were carried out on a SU-8220 instrument. Energy dispersive X-ray (EDX) measurements were performed on a Quanta 200 instrument. Transmission electron microscopy (TEM) images and element mapping images were tested on a JEM-2800 microscope equipped with a dual EDX high-throughput energy spectrum detector. X-ray photoelectron spectroscopy (XPS) spectrum were tested on an Thermo Fisher Scientific escalab Xi+ spectrometer. To identify the composition of Rh_3-Au_1 CNSs, inductively coupled plasma atomic emission spectroscopy was performed on Prodigy 7.

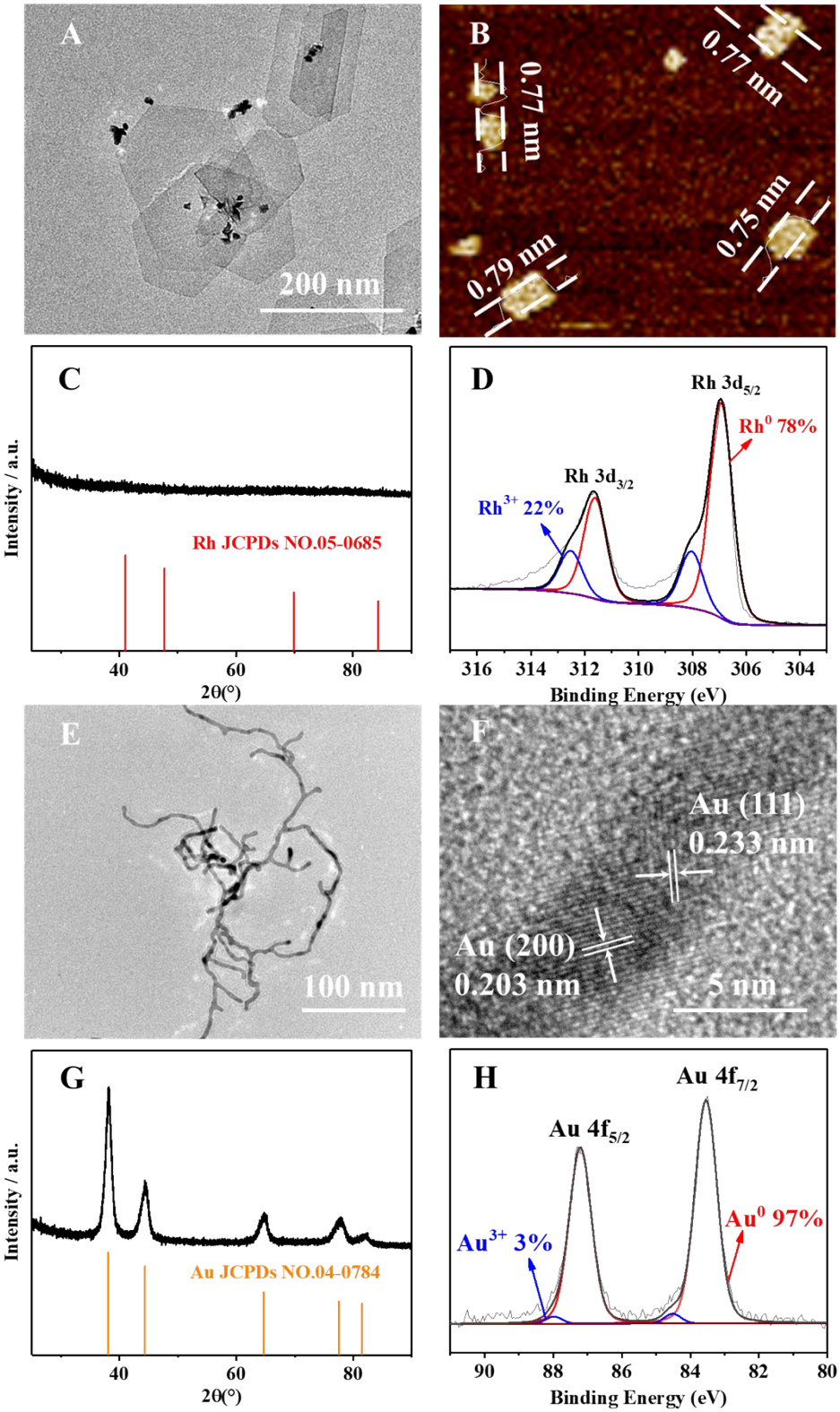

Fig. S1 (A) TEM image, (B) AFM image, (C) XRD pattern and (D) Rh 3d XPS spectrum of Rh NSs. (E) TEM image, (F) HRTEM image, (G) XRD pattern and (H) Au 4f XPS spectrum of Au NWs.

The morphology, crystal structure and atomic valence of as-prepared Rh NSs and Au NWs were characterized by TEM, AFM, XRD and XPS. First of all, TEM image shows

the 2D sheet-like structure of Rh NSs with an edge length of approximately 200 nm (Fig. S1A). AFM image reveals that the typical thickness of Rh NSs is 0.77 nm, suggesting an ultrathin structure (Fig. S1B). Concurrently, XRD pattern of Rh NSs shows no discernible diffraction peaks, which is directly related to the ultrathin 2D nature (Fig. S1C). XPS analysis results of Rh NSs demonstrate that the peak intensities of Rh^0 (307.0 and 311.7 eV) are higher than that of Rh^{3+} (308.0 and 312.5 eV), suggesting the majority of metallic Rh (Fig. S1D). In parallel, for Au NWs, TEM image confirms the well-defined 1D wavy nanowires with the average diameter of ca. 5 nm (Fig. S1E). The high-resolution TEM (HRTEM) image shows that the lattice spacing is 0.233 nm, corresponding to the {111} lattice spacing of face-centered cubic Au (JCPDS-04-0784, Fig. S1F). Moreover, XRD pattern of Au NWs matches well with the reflections of face-centered cubic Au (JCPDS-04-0784, Fig. S1G). Au 4f XPS spectrum reveals the peak intensities of Au^0 (83.5 and 87.2 eV) are much higher than that of Au^{3+} (84.5 and 88.0 eV), indicating that metallic Au is dominated species on the surface of Au NWs (Fig. S1H).

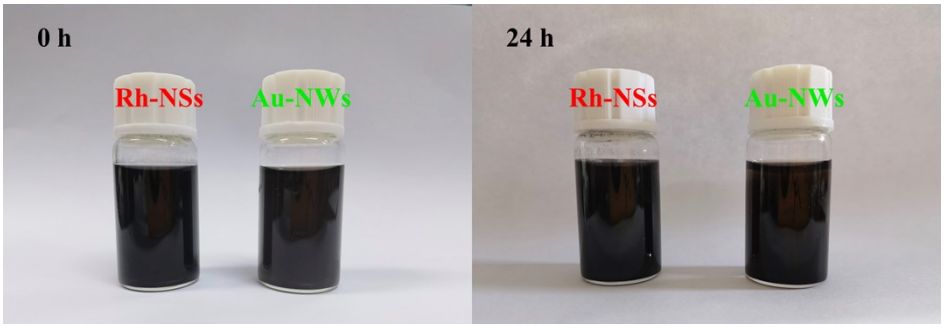

Fig. S2 Digital photos of Rh NSs and Au NWs dispersion in water.

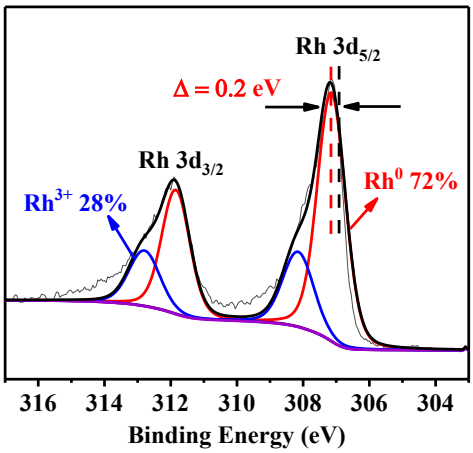

Fig. S3 Rh 3d XPS spectrum of Rh_3-Au_1 CNSs (The black vertical dotted line shows the standard XPS data).

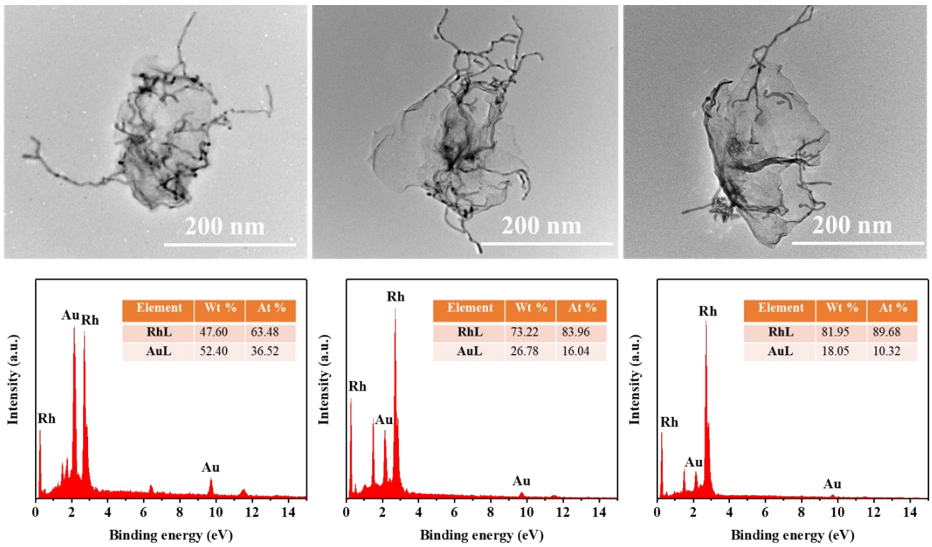

Fig. S4 TEM images and EDX spectra of Rh_7-Au_4 CNSs, Rh_5-Au_1 CNSs and Rh_9-Au_1 CNSs.

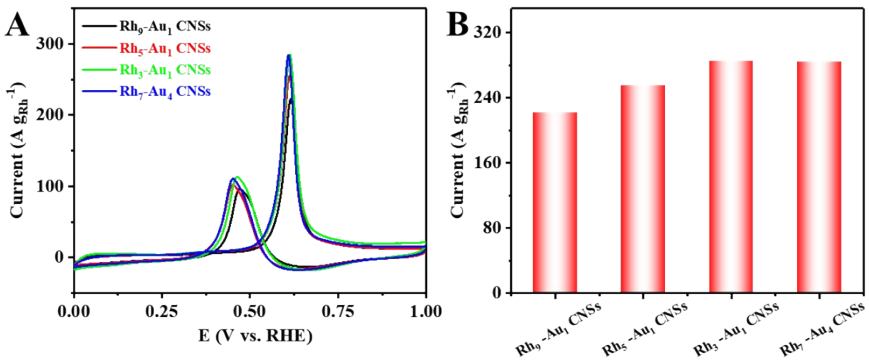

Fig. S5 (A) CV curves of Rh_7-Au_4 CNSs, Rh_3-Au_1 CNSs, Rh_5-Au_1 CNSs and Rh_9-Au_1 CNSs in N_2-saturated 1 M KOH + 0.5 M methanol solution at 50 mV s^{-1}. (B) MOR activities of Rh_7-Au_4 CNSs, Rh_3-Au_1 CNSs, Rh_5-Au_1 CNSs and Rh_9-Au_1 CNSs.

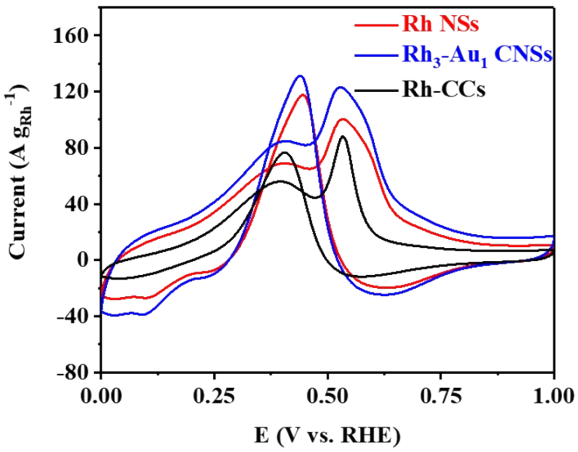

Fig. S6 CV curves of Rh_3-Au_1 CNSs, Rh NSs and Rh-CCs in N_2-saturated 5 M formate + 3 M KOH solution at 50 mV s^{-1}.

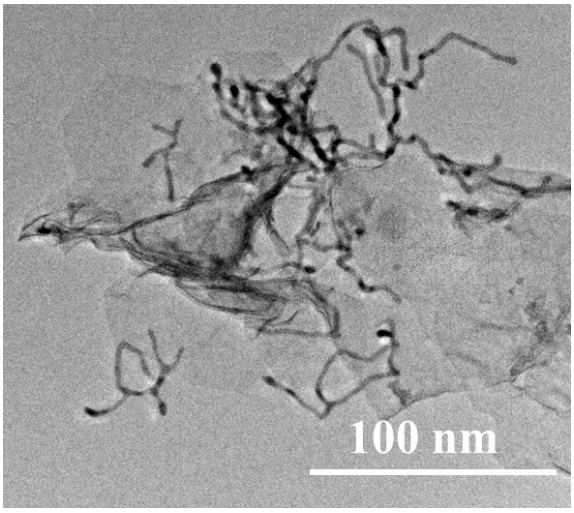

Fig. S7 TEM image of Rh_3-Au_1 CNSs after the stability test.

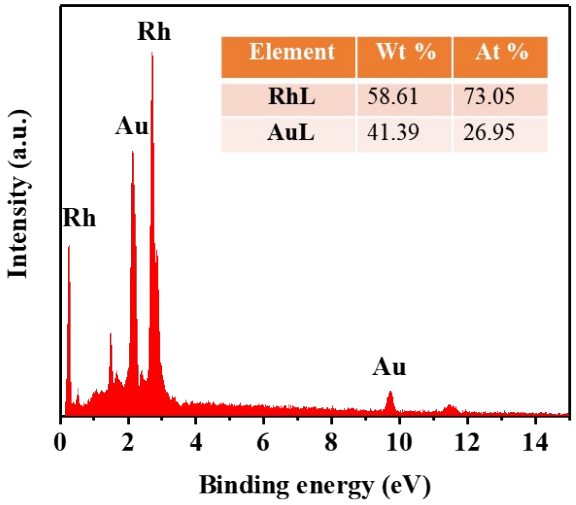

Fig. S8 EDX spectrum of Rh_3-Au_1 CNSs after the stability test.